JCSE The Journal of Corrosion Science and Engineering

ISSN 1466-8858 Volume 19, Paper 74 first submitted 31 December 1969
published 31 December 1969

Evaluation of steel corrosion inhibition by aluminium dihydric tripolyphosphate and calcium oxide using electrochemical methods and SEM technologies

Weiqiang Song [1]*, *Qinghuan Song* [2], *Longchao Wu* [1], *and Lantao Yang* [1]

[1] *School of Materials Science and Engineering, Henan University of Technology, Zhengzhou, China 450001;*

[2] *Medical Physics Laboratory, Luohe Medical College, Luohe, China 462003.*

*Corresponding author: Weiqiang Song
Telephone: +86 18623719057; +86 371 67758729
Email: weiqiang_song@haut.edu.cn
Full postal address: 100 Lianhua Road, Zhengzhou Hi-tech development Zone, 450001, P. R. China

Abstract

Corrosion inhibition of aluminium dihydric tripolyphosphate (ADTP) alone and in combination with CaO was evaluated using electrochemical methods and scanning electron microscope technologies. The inhibition of ADTP/CaO was superior to that of ADTP alone, but decreased with time, which revealed no contribution to the long-term effect. Furtherly, an equivalent circuit of $R_s(Q_1(R_1(Q_2(R_2W))))$ was given. The microcracks in the protective film formed on the surface should be responsible for the inferior inhibitive ability.

KEY WORDS: aluminium dihydric tripolyphosphate, calcium oxide, corrosion inhibition, electrochemical method, scanning electron microscope.

INTRODUCTION

Corrosion is a gradual destruction of materials (usually metals) by chemical and/or electrochemical reaction with the corrosive agents in their environment. The corrosive agents are generally oxygen, hydrogen sulfide, and carbon dioxide.[1-4] A common mechanism for inhibiting corrosion involves formation of a coating, often a passivation layer, which prevents access of the corrosive substance to the metal. In order to enhance the barrier effect, anticorrosive pigments are essentially incorporated in the coatings. Some toxic inorganic pigments containing chromium, lead, cadmium and so on, like chrome yellow, zinc yellow and lead red, are not generally considered inhibitors, however. A new generation of pigments, such as phosphates of zinc, molybdenum, calcium and aluminum, have been suggested and used widely as environmentally friendly alternatives.[5,6] As one of the important anti-corrosive pigments, aluminium dihydric tripolyphosphate (ADTP) has a multi-layered configuration with the terminal hydroxyl groups connecting to PO_4 units. The hydroxyl groups protrude into the inter-lamellar region and hydrogen bond with the inter-lamellar water molecules which in turn holds the layers and structure together.[7] The presence of the terminal hydroxyl groups makes ADTP have strong acidity, and accordingly, ADTP tends to display generally inferior corrosion inhibition. Among strategies developed to improve the performance of ADTP, modification of the surface of ADTP with metal oxides is an effective method. [8-10] In the present study, the corrosion inhibition performance of ADTP and CaO-neutralized ADTP was evaluated by electrochemical impedance spectroscopy (EIS) technology.

Experimental

Materials

Alumina oxide, calcium oxide, phosphoric acid and sodium chloride were purchased from Shanghai Aladdin Industrial Corporation. In a typical procedure, aluminum hydroxide slurry and phosphoric acid solution (mole ratio of P_2O_5 / Al_2O_3 is 3:1) was mixed at 90 °C in a container. The container was stirred at 100 °C for 1.5 hours and the mixture turned to translucent viscous slurry. The slurry was immediately placed into a reacting furnace set at 310 °C. After reacting for 10 hours, the obtained solid was taken out of the furnace and immersed in distilled water. After hydration reaction, the product was treated by dehydration drying and further crushing. X-ray diffraction (XRD) studies revealed a coexistence of two main structural phases, ADTP and $AlPO_4$ in the product. The product was not further separated and purified.

X-ray diffraction

The X-ray diffraction (XRD) spectrum of the previous product (equilibrated at 100% relative humidity, at 25 °C for 48 h) was recorded using an Analytical Diffractometer (Bruker D8 Advance), Cu Kα radiation with a wave length of 0.154 nm operating at 40 kV and 35 mA (as shown in Fig.1).

Electrochemical measurements

JCSE The Journal of Corrosion Science and Engineering
ISSN 1466-8858 Volume 19, Paper 74 first submitted 31 December 1969
published 31 December 1969

Tinplate panels (120 × 50 × 0.28mm) were pre-treated by mechanical cleaning (polishing), degreasing in an acetone solution and rinsing with distilled water. In order to prepare ADTP extracts, 0.2g of each portion was stirred in 100ml 3.5% w/w NaCl aqueous solution for 24 h.

EIS measurements were carried out in RST5200F electrochemical working instrument (Zhengzhou shiruisi Instrument Technology Co., Ltd.), in the frequency range of 100000 Hz to 0.001 Hz, using perturbation amplitude of 5mV around the open circuit potential. The electrochemical cell with a three-electrode configuration including Ag/AgCl reference electrode (RE), the tinplate sheet as the working electrode (WE) and platinum counter electrode (CE) was used to run the tests. A working face of 1cm^2 area was left on the surface of the tinplate panels. Three replicate panels were conducted to ensure repeatability.

Surface analysis

The surface of the test panels after exposure to 3.5% NaCl solution in the presence of ADTP and CaO was examined by scanning electron microscopy (SEM). Before the examination, the panels were washed with double distilled water and dried in dry condition. An Inspect F50 Scanning Electron Microscope was operated at an accelerating voltage of 20 kV and an 18 mm working distance.

Results and discussions

EIS measurement in the presence of ADTP alone

The studied ADTP was synthesized from aluminum hydroxide slurry and phosphoric acid solution (mole ratio of P_2O_5 / Al_2O_3 is 3:1). The XRD spectrum of the product is shown in Fig. 1.

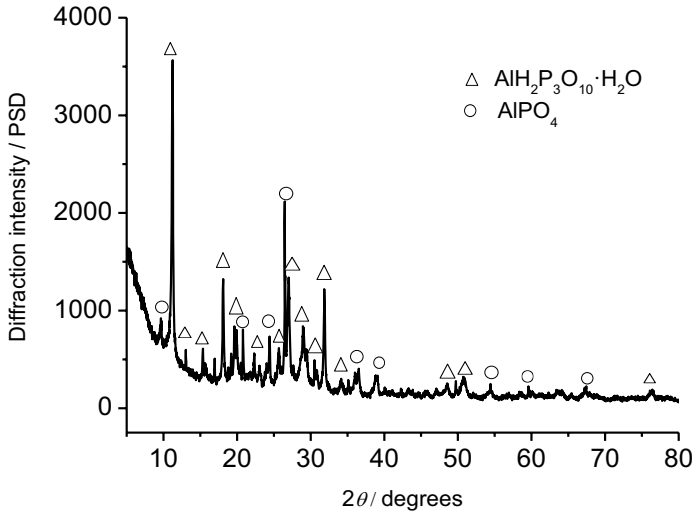

Fig. 1. *XRD spectrum of ADTP in the present study.*

The spectrum indicates that the product is mainly composed of ADTP. The representative Nyquist and Bode plots of tinplate panels obtained in aqueous ADTP suspensions prepared by 3.5% NaCl solution after different times of immersion are shown in Fig. 2. As shown in Fig.2 (A), each of the Nyquist plots exhibits an obvious capacitive loop in the high frequency region and a straight-line tail at low frequencies. The following tail at low frequencies is commonly called as Warburg's impedance, which implies that the corrosion of steel in ADTP suspensions is diffusion controlled. The high frequency loop is related to charge transfer resistance, which indicates that the corrosion reaction is controlled by charge transfer process. The diameter of capacitive loop more and more increased as the time elapsed in 120 hours, which indicates the adsorption process of inhibitor molecules on the metal surface. The adsorption results in an increase of polarization resistance and reduces the corrosion rate of the tested panel, which indicates a corrosion inhibition effect of ADTP on the surface of the tested steel panels. [11,12] But it is carefully observed that the imaginary part of the resistance is higher after immersion for 24 hours at low frequencies as shown in Fig. 2 (A) and accordingly the resistance is higher at low frequencies below 2.2×10^{-2} *Hz* as shown in Fig. 2 (B). This can be attributed to a greater contribution of the reactance. In addition, the low-frequency impedance is constituted by a horizontal straight line at relatively low frequencies after immersion for 2 hours and 120 hours as shown in Fig. 2 (B), while by an oblique line after immersion for 24 hours. The straight line at low frequencies implies that the corrosion of the steel panel in 3.5% NaCl in the presence of ADTP is diffusion controlled. The diffusion process may be due to the transportation of corrosive ions and soluble corrosion products at the metal/solution interface.

JCSE The Journal of Corrosion Science and Engineering
ISSN 1466-8858 Volume 19, Paper 74 first submitted 31 December 1969
published 31 December 1969

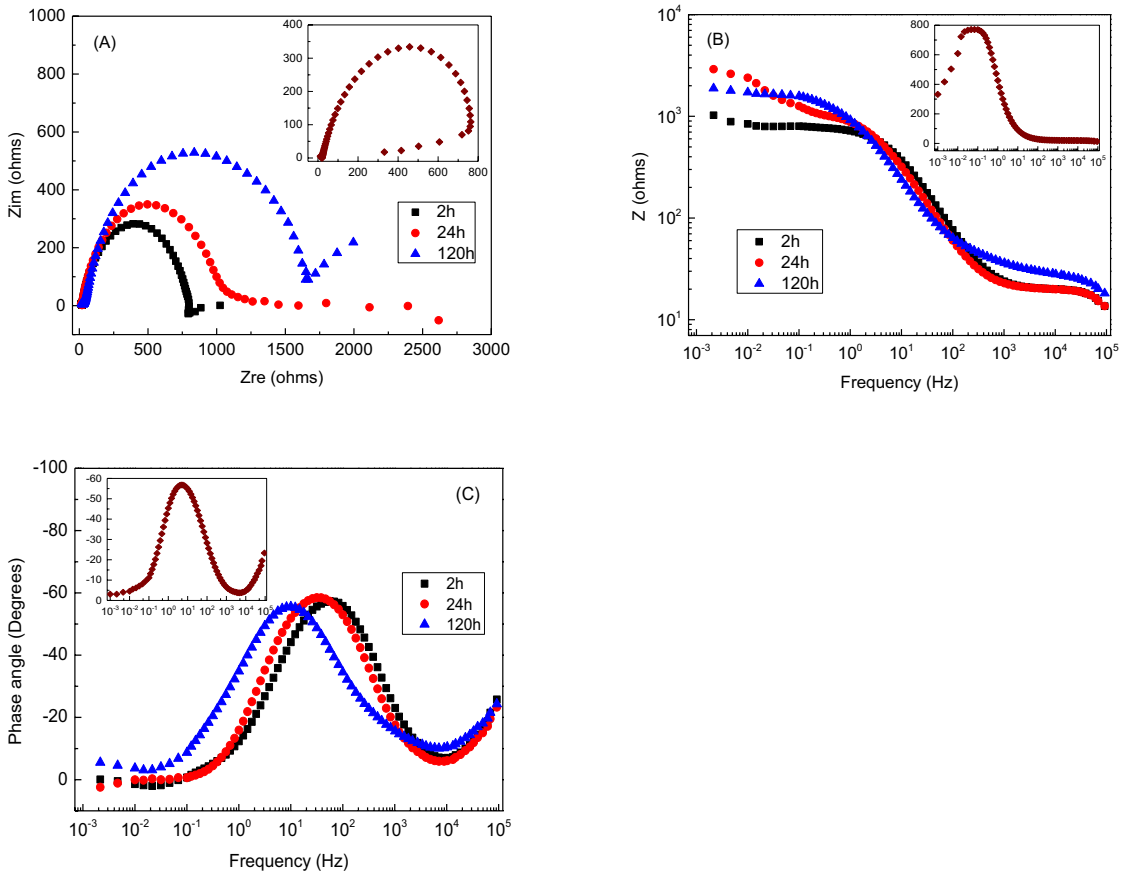

Fig. 2. *Nyquist plots (A) and Bode plots (B) and (C) obtained for tinplate steel panels in 3.5% NaCl solutions in the presence of ADTP alone after immersion for 2h, 24h and 120h, respectively. The inset plots were obtained for tinplate steel panels in 3.5% NaCl solutions in the absence of ADTP.*

In literatures, the protective mechanism of ADTP for steel is proposed as follows: When it is dissolved in aqueous solution, the tri-phosphoric ion ($P_3O_{10}^{5-}$) is formed, which exhibits strong chelation ability and can chelate with various metal ions, such as ferrous iron and ferric iron. The protective film formed by chelates on the metal surface is stable, and can provide protective effect.

$$AlH_2P_3O_{10} \rightarrow Al^{3+} + 2H^+ + P_3O_{10}^{5-}$$

$$Fe^{2+} + Fe^{3+} + P_3O_{10}^{5-} \rightarrow Fe_2P_3O_{10}$$

Even if $P_3O_{10}^{5-}$ depolymerized, the formed orthophosphate ion (PO_4^{3-}) can also construct protective film.

$$P_3O_{10}^{5-} + 2H_2O \rightarrow 3PO_4^{3-} + 4H^+$$

$$x\left(Fe^{2+},\ Fe^{3+}\right) + yPO_4^{3-} \rightarrow Fe_x\left(PO_4\right)_y$$

Based on the protective mechanism and the data fitting, EIS diagrams shown in Fig. 2 were analyzed using the equivalent circuit (EC) displayed in Fig. 3.

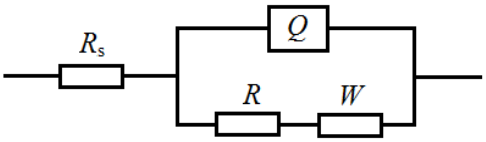

Fig. 3. *Equivalent circuit used to simulate the experimental plots displayed in Fig. 2.*

The proposed EC is given by $R_s(Q(RW))$, where R_s is the solution resistance between the working and the reference electrodes; Q is the constant-phase element (CPE); R is the charge-transfer resistance in connection with a Warburg element; W is Warburg's impedance.

JCSE The Journal of Corrosion Science and Engineering
ISSN 1466-8858 Volume 19, Paper 74 first submitted 31 December 1969
published 31 December 1969

The starting point of the capacitive loop at high frequencies almost coincides with zero point as shown in Fig. 2 (A), indicating R_s is very small. *Q* indicates the process of semi-infinite diffusion, which can be treated as an imperfect semipermeable capacitor.

In theory, the AC impedance (Z) of the electrode is composed of real and imaginary parts. According to EC as shown in Fig. 3, Z can be expressed as follows.

$$Z = R_s + \frac{a}{b^2 + \omega^2 C_d^2 a^2} - j\frac{\omega C_d a^2 + \sigma\omega^{-\frac{1}{2}} b}{b^2 + \omega^2 C_d^2 a^2} \qquad (1)$$

where $a = R_{ct} + \sigma\omega^{-\frac{1}{2}}$, $b = 1 + C_d\sigma\omega^{\frac{1}{2}}$ and σ is Warburg coefficient, which is related with diffusion coefficients and concentrations. Warburg's resistance is expressed as follows.

$$R = \frac{1}{\omega C_W} = \sigma\omega^{-\frac{1}{2}} \qquad (2)$$

As known, the anodic dissolution of steel takes place in parallel with the cathodic reduction of oxygen on the panel surface. Consequently, the diffusion process is due to either the transportation of corrosive ions and soluble corrosion products at the steel/solution surface or the diffusion of dissolved oxygen to the steel surface. However, oxygen diffusion control is more reasonable. σ can be expressed as follows.

$$\sigma = \frac{RT}{\sqrt{2D_O}n^2F^2c_O^o} \qquad (3)$$

where D_O and C_O^o are oxygen's diffusion coefficient and concentration, respectively.

At high frequencies, Warburg's resistance is low, and concentration polarization could be ignored. Accordingly, Equation (1) is simplified as the following equation.

$$Z = R_s + \frac{R_{ct}}{1 + \omega^2 C_d^2 a^2} - j\frac{\omega C_d R_{ct}^2}{1 + \omega^2 C_d^2 R_{ct}^2} \qquad (4)$$

$$\left(Z' - R_s - \frac{R_{ct}}{2}\right)^2 + \left(-Z''\right)^2 = \left(\frac{R_{ct}}{2}\right)^2 \qquad (5)$$

So, R_s, R_{ct} and C_d could be obtained from the data at high frequencies in Fig. 2 (a) according to Equation (5). Based on the semi-circle of the Nyquist plot, the coordinate of the center is $\left(R_s + \frac{R_{ct}}{2}\right)$ and the diameter is equal to R_{ct}. The capacitance of electric double layer can be calculated according to the frequency determined at the apex of the semi-circle, that is, $\omega^* = \frac{1}{R_{ct}C_d}$.

Moreover, when the frequency is low enough to result in b approaching 1, $\omega^{\frac{1}{2}}$, ω and ω^2 could be reasonably neglected, and then the following equation is derived.

$$Z = R_s + R_{ct} + \sigma\omega^{-\frac{1}{2}} - j(2C_d\sigma^2 + \sigma\omega^{-\frac{1}{2}}) \qquad (6)$$

So,

$$Z' = R_s + R_{ct} + \sigma\omega^{-\frac{1}{2}} \qquad (7)$$

$$-Z'' = 2C_d\sigma^2 + \sigma\omega^{-\frac{1}{2}} \qquad (8)$$

Equation (6) and (7) are combined into the following Equation (9).

$$Z' = R_s + R_{ct} - 2C_d\sigma^2 + (-Z'') \qquad (9)$$

JCSE The Journal of Corrosion Science and Engineering
ISSN 1466-8858 Volume 19, Paper 74 first submitted 31 December 1969
published 31 December 1969

In the $Z' \sim Z''$ diagram as shown in Fig. 1 (a) for 120 h of immersion, the intercept on the Z' axis is $R_s + R_{ct} - 2C_d\sigma^2$, and the slope is obviously equal to -1. Based on R_s, R_{ct} and C_d obtained from the data in the high frequency region, the Warburg coefficient σ is obtained. Different from the theoretical description, the slopes of the straight-line tails at low frequencies for 2h and 24h of immersion deviate from -1, which indicates that the Warburg's impedance is affected by more factors besides oxygen diffusion.
As for the bode plots in Fig. 2 (b) and (c), the concentration polarization can be ignored in the high frequency region, which results in $|Z| \to 0$, $tg(-\theta) \to 0$ and $\theta \to 0$. In the middle frequency region, the role of the capacitive component in the system is gradually obvious, and the slope of $\log|Z| \sim \log f$ is -1 under the condition of ignoring the concentration polarization. In the low frequency region, the concentration polarization dominates, and R_s and R_{ct} are relatively low enough to be ignored. Furthermore, in the equivalent circuit can be ignored in the very low frequency region. Equation (6) is simplified as the following equation.

$$Z = \sigma\omega^{-\frac{1}{2}} - j\sigma\omega^{-\frac{1}{2}} \qquad (10)$$

In this case, $(\omega C_d)^{-1}$ is attributed to the capacitance of electric double layer capacitor, and $\sigma\omega^{-\frac{1}{2}}$ is attributed to Warburg's resistance. The following equation is extended.

$$\log|Z| = \log\sigma\omega^{-\frac{1}{2}} + \log\sqrt{2} = \log\frac{\sigma}{\sqrt{\pi}} - \frac{1}{2}\log f \qquad (11)$$

So, the slope of $\log|Z| \sim \log f$ is $-\frac{1}{2}$.

In view of the presence of the Warburg's resistance, $Z' \sim \omega^{-\frac{1}{2}}$ and $-Z'' \sim \omega^{-\frac{1}{2}}$ plots are shown in Fig.1(d). $Z' \sim \omega^{-\frac{1}{2}}$ in the low frequency region is shown as a straight line according to Equation (6), and the intercept of the linear extrapolation to $Z' = 0$ gives $(R_s + R_{ct})$. Similarly, $-Z''$ is linear with $\omega^{-\frac{1}{2}}$ according to Equation (7) in the low frequency region, the slope of the straight line is equal to σ and the intercept of the linear extrapolation to $-Z'' = 0$ gives $2C_d\sigma^2$.
The difference in real impedance at lower and higher frequencies is commonly taken as a charge transfer resistance in analysis of Nyquist data. [13] In case of the difference taken as the polarization resistance (R_p), the corresponding inhibition efficiency (η) of ADTP could be calculated using the following equation:

$$\eta = \left(1 - \frac{R_p^0}{R_p}\right) \times 100\% \qquad (12)$$

where R_p^0 and R_p are polarization resistances in the absence and presence of ADTP, respectively. η calculated for 2, 24 and 120 hours of immersion is 3.14%, 30.79% and 53.58%, respectively.

EIS measurement in the presence of ADTP/CaO

The previous EIS results showed that ADTP is not sufficient to inhibit corrosion of the tinplate steel. The inferior ability of ADTP in corrosion inhibition is usually attributed to its acidity. In the present study, alkaline CaO was used to offset the acidity of ADTP.
The electrochemical behavior for the steel panels in the presence of ADTP/CaO in 3.5% NaCl solutions were investigated and corresponding EIS plots are shown in Fig. 4.

JCSE The Journal of Corrosion Science and Engineering
ISSN 1466-8858 Volume 19, Paper 74 first submitted 31 December 1969
published 31 December 1969

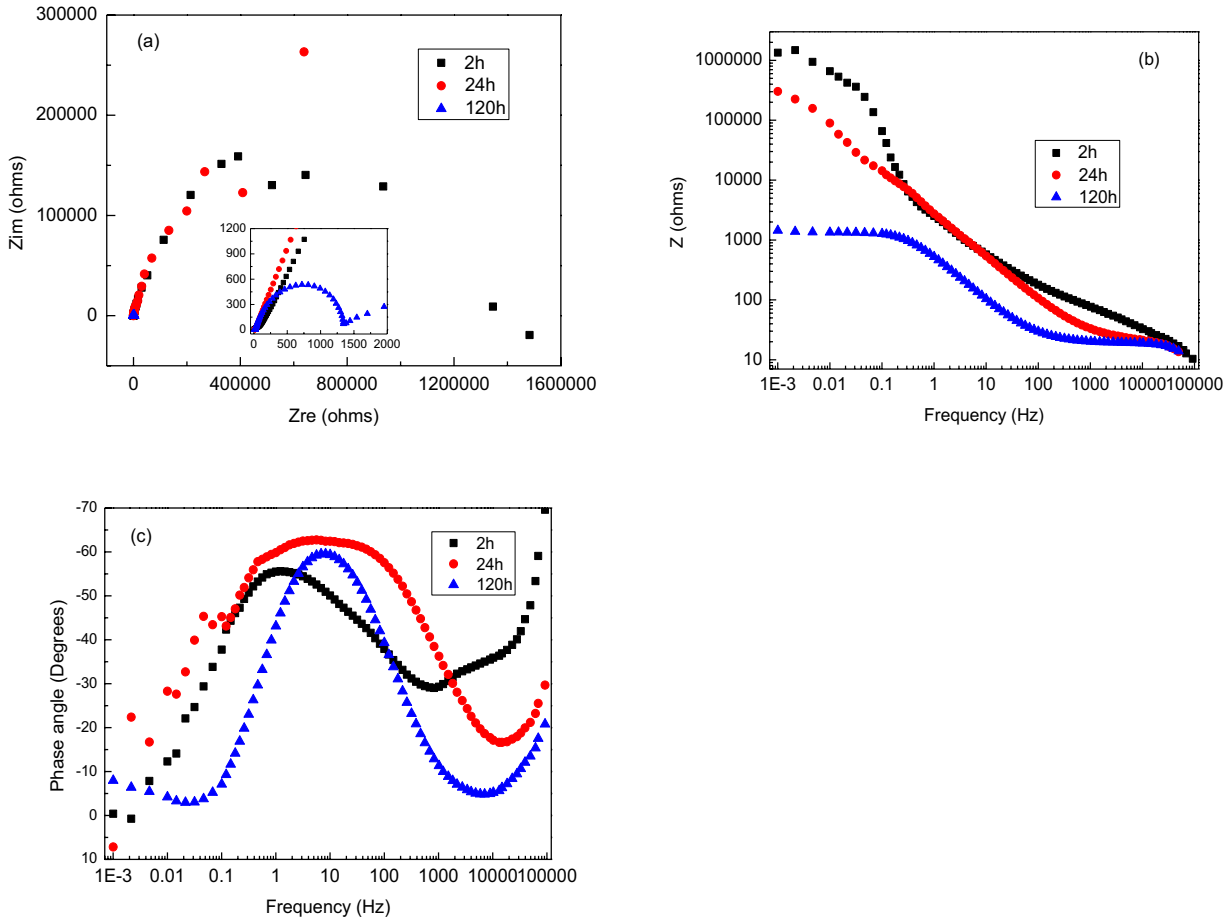

Fig. 4. *Nyquist plots (a) and Bode plots (b and c) obtained for tinplate steel panels in 3.5% NaCl solutions in the presence of ADTP/CaO after 2h, 24h and 120h of immersion*.

Compared with EIS diagrams in Fig. 2, there are three points that need to be pointed out for EIS diagrams in Fig. 4. The first is, at low frequencies, |Z| in Fig. 4 is three orders higher than that in Fig. 2 for 2 and 24 hours of immersion, which indicates enhanced corrosion inhibition effect of ADTP/CaO. The second is, in particular, the EIS diagrams in Fig. 4 for 120 hours of immersion is very similar to those in Fig. 2 for 120 hours of immersion, which indicates a similar electrochemical behavior after long time of immersion. The third is, |Z| decreased as the time elapsed in 120 hours. The EIS data reveals that CaO can significantly enhance the corrosion inhibition effect of ADTP on tinplate steel during short-term immersion, whereas no contribution to the long-term effect. η for 2, 24 and 120 hours of immersion in the presence of ADTP/CaO is 99.95%, 99.93% and 42.76%, respectively, which indicates that in the short term CaO can significantly improve the ability of ADTP to inhibit the corrosion of steel, but in the long term CaO may not effectively improve the ability. Or, more accurately, the presence of CaO is harmful to the ability of ADTP to inhibit corrosion in the long term. For example, after immersion of 120 hours, η is 53.58% in the presence of ADTP and is 42.76% in the presence of ADTP/CaO, respectively.

The frequency corresponding to the maximum phase angle cover a wide range for 2 and 24 hours of immersion in Fig. 4 (c), which is commonly taken as a good performance of passive film protection in some passivation systems. The wide range can mean the superposition of two time constants. The additional time constant can be attributed to the formation of $CaAlP_3O_{10}$ film.

$$AlH_2P_3O_{10} + CaO \rightarrow CaAlP_3O_{10} + H_2O$$

$$CaAlP_3O_{10} \leftrightarrow Ca^{2+} + Al^{3+} + P_3O_{10}^{5-}$$

EIS diagrams for immersion of 2 and 24 hours shown in Fig. 4 were analyzed using EC displayed in Fig. 5. The proposed EC is given by $R_s(Q_1(R_1(Q_2(R_2W))))$. Otherwise, EIS diagrams for immersion of 120 hours were simulated by EC shown in Fig. 2.

JCSE The Journal of Corrosion Science and Engineering
ISSN 1466-8858 Volume 19, Paper 74 first submitted 31 December 1969
published 31 December 1969

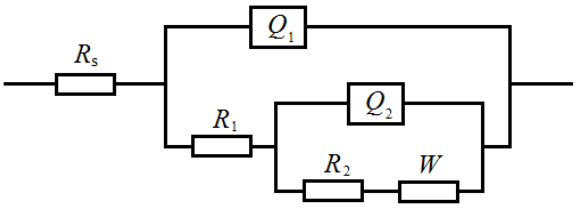

Fig. 5. *Equivalent circuit used to simulate the experimental plots for immersion of 2 and 24 hours displayed in Fig. 4.*

Tafel polarization measurement

The Tafel polarization curves for tinplate panels in 3.5% NaCl solutions in the presence of ADTP alone and ADTP/CaO after immersion of 2, 24 and 120 hours, are shown in Fig. 6 and Fig. 7, respectively. From these curves, the corrosion current density (i_{corr}), the corrosion potential (E_{corr}) and the cathodic Tafel slope (β_c) as obtained are listed in Table 1. Additionally, the corrosion current density was determined by extrapolation of the cathodic branch to the corrosion potential. The inhibition efficiency (η_{Tafel}) was calculated using Eq. (13).

$$\eta_{Tafel} = \frac{i^0_{corr} - i_{corr}}{i^0_{corr}} \times 100\% \qquad (13)$$

Where i_{corr} is the corrosion current density in the presence of ADTP, and i^0_{corr} the corrosion current density in the absence of ADTP.

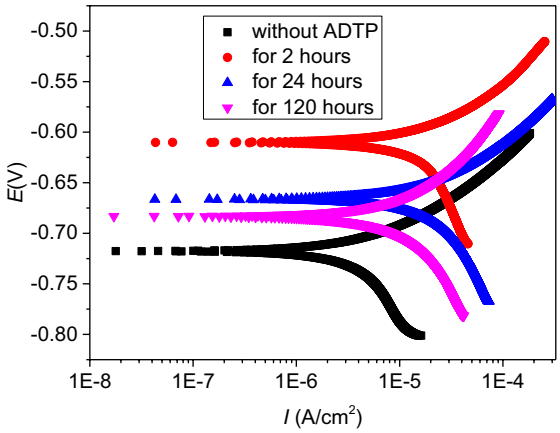

Fig. 6. *Tafel polarization curves of tinplate panels in 3.5% NaCl solution after immersion of 2, 24 and 120 hours in the presence of ADTP alone, respectively, and the curve in the absence of ADTP.*

JCSE The Journal of Corrosion Science and Engineering
ISSN 1466-8858 Volume 19, Paper 74 first submitted 31 December 1969
published 31 December 1969

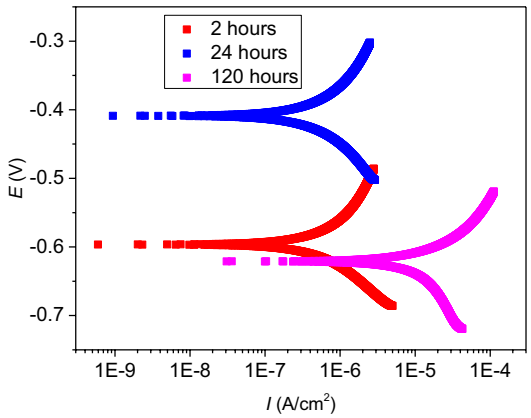

Fig. 7. *Tafel polarization curves of tinplate panels in 3.5% NaCl solution after immersion of 2, 24 and 120 hours in the presence of ADTP/CaO.*

Table 1. Some Tafel parameter values for tinplate panels in 3.5% NaCl solution

Type of testing solution	E_{corr} (V)	i_{corr} (μA/cm²)	β_c (mV/dec)	η_{Tafel}
Without ADTP	-0.733	4.63	166	0
ADTP, for 2 hours	-0.611	22.2	241	<0
ADTP, for 24 hours	-0.667	21.9	208	<0
ADTP, for 120 hours	-0.689	12.8	182	<0
ADTP/CaO, for 2 hours	-0.598	0. 728	91.6	84.3%
ADTP/CaO, for 24 hours	-0.411	0. 606	128	86.9%
ADTP/CaO, for 120 hours	-0.644	15.3	196	<0

The results show that i_{corr} in the presence of ADTP alone was higher than that in the absence of ADTP, and decreased gradually with time after immersion. From Table 1, it can be noted that i_{corr} in the presence of ADTP/CaO after immersion of 2 and 24 hours occurs almost seven times less than that in the absence of ADTP. The measurement of less i_{corr} shows that ADTP/CaO has barrier property toward diffusive ions.

SEM of the tinplate surfaces after immersion

SEM micrograph of the tested tinplate surface after immersion of 120 hours in the presence of ADTP alone is shown in Fig. 8. The figure shows that the protective film is formed on the surface, but it is not integrated. The inferior corrosion inhibition can be attributed to the broken protective film.

JCSE The Journal of Corrosion Science and Engineering
ISSN 1466-8858 Volume 19, Paper 74 first submitted 31 December 1969
published 31 December 1969

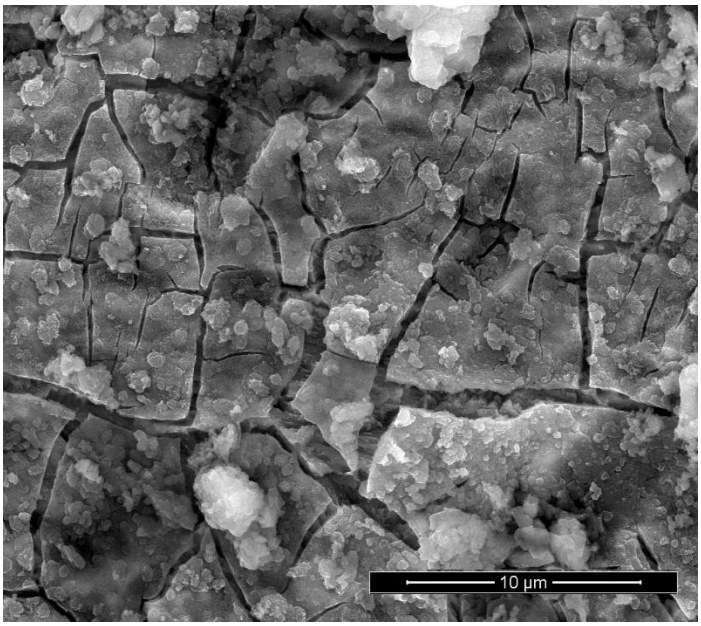

Fig. 8. *SEM micrograph of the tinplate surface in the presence of ADTP alone after immersion of 120 hours.*

SEM micrographs after immersion of 2, 24 and 120 hours in the presence of ADTP/CaO are shown in Fig. 9. Fig. 9 (A) and (B) show that the protective films after immersion of 2 and 24 hours are relatively integrated, and there are not gap in the films, which is the reason why the corrosion inhibition performance is good. Similarly to Fig. 8, Fig. 9 (C) shows a broken protective film.

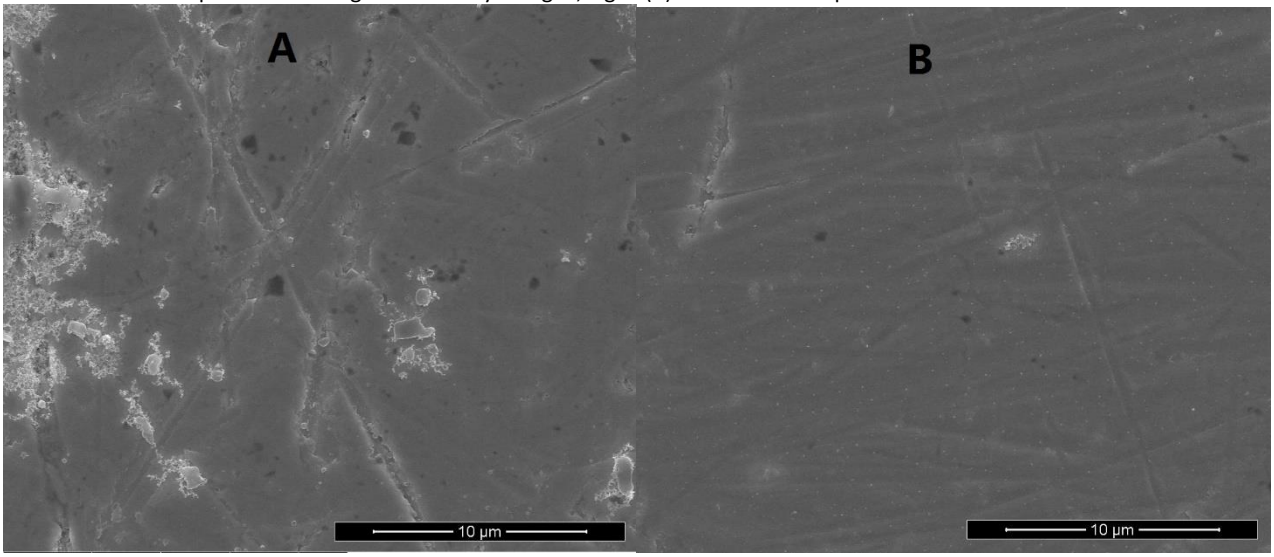

JCSE The Journal of Corrosion Science and Engineering
ISSN 1466-8858 Volume 19, Paper 74 first submitted 31 December 1969
published 31 December 1969

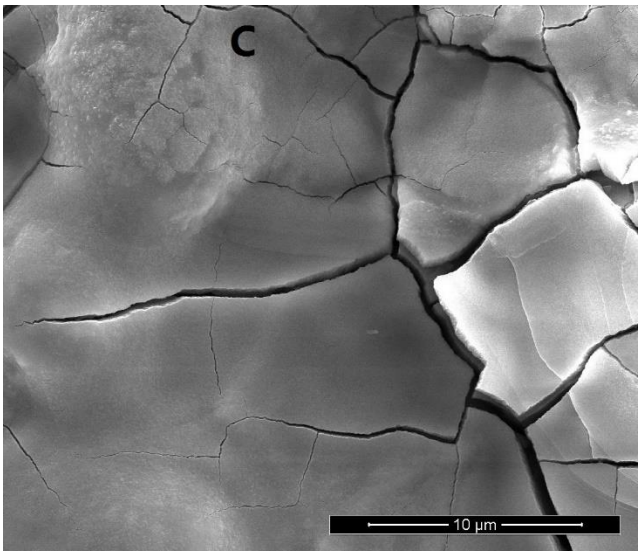

Fig. 9. *SEM micrograms of the tinplate surfaces in the presence of ADTP/CaO after immersion of 2 (A), 24 (B) and 120 (C) hours.*

Conclusion

In the presence of ADTP alone, the ability for ADTP inhibiting steel corrosion increased with time, but its inhibitive efficiency is inferior. The inferior corrosion inhibition can be attributed to the broken protective film formed on the surface of the tested tinplate panels. The Warburg's impedance is affected by more factors besides oxygen diffusion, which attributed to the deviation from the theoretical description.

In the presence of ADTP/CaO, the inhibitive ability decreased with time, but it is better than that of ADTP alone after immersion of 2 and 24 hours, which is attributed to the integrated film formed on the surface of tinplate panels. After immersion of 120 hours, the protected film is broken and the inhibitive ability becomes poor, which is similar to that of ADTP alone. The electrochemical results are completely in agreement with the morphological results of the surface obtained from SEM micrograph. CaO as an alkaline filler can improve the anticorrosive efficiency of ADTP, but it is not effective in long term.

Acknowledgments

This study was supported by the Provincial Scientific Project of Henan (Grant no. 152102210069) and the Science and Technology Innovation Team Project of Zhengzhou City (Grant no. 131PCXTD615)

No conflict of interest exits in the submission of this manuscript.

References

[1] 'Corrosion of deicers to metals in transportation infrastructure: introduction and recent developments: corrosion reviews', X. Shi, L. Fay, Z. Yang, T. A. Nguyen, Y. Liu, *Corros. Rev.*, 27, 27, pp.23-52, 2011.

[2] 'Development of an effective method for internal pipeline corrosion control in the presence of CO_2', I. Jevremovic, M. Singer, M. Achour, S. Nesic, V. Miskovic-Stankovic, *Zastita Materijala,* 57, 2, pp.195-204, 2016.

[3] 'Oxygen Distribution as a Factor in the Corrosion of Metals', U. R. Evans, *Ind. Eng. Chem.*, 17, pp 363-372, 2002.

[4] 'An electrochemical model for prediction of corrosion of mild steel in aqueous carbon dioxide solutions', S. Nesic, J. Postlethwaite, S. Olsen, *Corrosion,* 52, 13, pp280-294, 2013.

[5] 'Evaluation of anti-corrosive pigments by pigment extract studies, atmospheric exposure and electrochemical impedance spectroscopy', A. Amirudin, C. Barreau, R. Hellouin, D. Thierry, *Prog. Org. Coat.*, 25, 4, pp339-355, 1995.

[6] 'A Comparison Study on Corrosion Behavior of Zinc Phosphate and Potassium Zinc Phosphate Anticorrosive Pigments', E. Alibakhshi, E. Ghasemi, M. Mahdavian, *Prog. Color. Colorants. Coat.,* 5 p. 91-99 (2012).

[7] 'Studies into the ion exchange and intercalation properties of $AlH_2P_3O_{10}•2H_2O$', T. P. Marsh, University of Birmingham, Birmingham, 2011.

[8] 'The inhibitive performance of polyphosphate-based anticorrosion pigments using electrochemical techniques', R. Naderi, M. M. Attar, *Dye Pigments*, 80, 3, pp349-354, 2009.

[9] 'Influence of anticorrosion pigments on protective properties of epoxy coatings', V. I. Pokhmurskyi, I. M. Zin, L. M. Bilyi, A. V. Vasylyk, *Mater. Sci.,* 36, 6, pp878-883, 2000.

[10] 'Aluminium tripolyphosphate pigments for anticorrosive paints', M. Deyá, V.F. Vetere, R. Romagnoli, B. del Amo, *Pigment Resin Tech.*, 30, 1, pp13-24, 2001.

[11] 'Inhibition of corrosion by several Schiff bases in aerated halide solutions', H. Ma, S. Chen, L. Niu, S. Zhao, S. Li, D. Li, *J. Appl. Electrochem.*, 32, pp65–72, 2002.

[12] 'Copper corrosion inhibition in O_2-saturated H_2SO_4 solutions', M. A. Amin, K. F. Khaled, *Corros. Sci.*, 52, pp1194–1204, 2010.

[13] 'The investigation of synergistic inhibition effect of rhodanine and iodide ion on the corrosion of copper in sulphuric acid solution', Solmaz, R., Şahin, E. A., Döner, A., & Kardaş, G., *Corrosion Science*, 53, 10, pp3231-3240, 2011.